FLOW MECHANISMS IN CREEP OF A SHORT-FIBRE AZ91 ALLOY-BASED COMPOSITE

†MARIE PAHUTOVÁ[1], VÁCLAV SKLENIČKA[1]*, KVĚTA KUCHAŘOVÁ[1], MILAN SVOBODA[1], TERENCE G. LANGDON[2]

[1] *Institute of Physics of Materials, Academy of Sciences of the Czech Republic, Žižkova 22, CZ-616 62 Brno, Czech Republic*
[2] *Departments of Aerospace & Mechanical Engineering and Materials Science, University of Southern California, Los Angeles, CA 90089-1452, USA*

Received 15 October 2004, accepted 16 November 2004

A comparison between the creep characteristics of an AZ91 magnesium alloy reinforced with 20 vol.% Al_2O_3 short fibres and an unreinforced AZ91 matrix alloy shows that the creep resistance of the reinforced material is considerably improved compared to the matrix alloy. It is suggested that the creep strengthening in the composite arises mainly from the existence of a threshold stress and the load transfer effect. The values of the threshold stress in the creep of the composite at temperatures in the range from 373 to 673 K were estimated using standard methods. It is proposed that the threshold stress arises from an attractive interaction between mobile dislocations and $Mg_{17}(Al,Zn)_{12}$ precipitates.

K e y w o r d s: AZ91 magnesium alloy, metal matrix composite, creep, short fibre reinforcement, threshold stress, load transfer effect

1. Introduction

The magnesium AZ91 alloy, containing aluminium and zinc as major alloying elements, has one of the best combinations of castability, mechanical strength and ductility of all the magnesium-based alloys. However, the creep resistance of this alloy is found to be rather limited at temperatures above 423 K. A considerable improvement in the creep properties of the AZ91 alloy can be potentially achieved through the incorporation of a non-metallic short-fibre reinforcement. Although a number of studies has been reported on the creep behaviour of the AZ91 monolithic alloy [1–13], the creep properties of short fibre reinforced AZ91-based composites

*corresponding author, e-mail: sklen@ipm.cz

have received only limited attention [5, 6, 9, 12, 14–20]. Recently, extensive examination of the creep properties of an AZ91 alloy reinforced with 20 vol.% Al_2O_3 short fibres and an unreinforced AZ91 matrix alloy were conducted [5, 12]. From these investigations it follows that the creep resistance of the reinforced alloy is considerably improved compared to the matrix alloy. The minimum creep rate for the composite is two to three orders of magnitude less than that of the unreinforced matrix alloy under the same loading conditions [6, 12]. Further, the creep life of the composite is an order of magnitude longer than that of the unreinforced alloy [12]. By contrast, the presence of the reinforcement leads to a substantial decrease in the creep plasticity [6].

At present it is generally accepted that creep deformation in metal matrix composites is controlled by flow in the matrix materials. This conclusion is supported by recent experimental results on the squeeze-cast AZ91-20vol.%Al_2O_3 short-fibre composite reported by Li et al. [15, 16]. When the creep data were interpreted by incorporation of a threshold stress σ_{TH} into the analysis, it was shown that the results are consistent with the behaviour anticipated for a magnesium solid solution alloys [21]. Thus, it can be suggested that the creep strengthening in the composite arises mainly from the existence of a threshold stress and/or the load transfer effect [17, 22].

This work reports additional experimental results obtained in an investigation of the high temperature creep behaviour of a fibre-reinforced AZ91 matrix composite and its matrix alloy. The objective of the present research is a further attempt to clarify the creep strengthening mechanisms in short-fibre reinforced magnesium alloys. Attention in this paper is focused primarily on the significance of the threshold stress and the load transfer effect in creep of the AZ91 composite.

2. Experimental materials and procedures

Unreinforced and short-fibre reinforced blocks of an AZ91 alloy (Mg-9wt.%Al--1wt.%Zn-0.3wt.%Mn) were fabricated by squeeze casting at the Department of Materials Engineering and Technology, Technical University of Clausthal, Germany. The fibre preform consisted of planar randomly distributed δ-alumina short fibres (Saffil fibres from ICI, 97 % Al_2O_3, 3 % SiO_2, ~ 3 μm in diameter with varying lengths up to an estimated maximum of ~ 150 μm). The final fibre fraction after squeeze casting in the composite was about 20 vol.%. For convenience, the composite is henceforth designated AZ91-20vol.%Al_2O_3(f), where f denotes fibre. Both materials were subjected to a standard T6 heat treatment (anneal for 24 h at 688 K, air cool and then age for 24 h at 443 K).

Flat tensile creep specimens, having gauge lengths of 25 mm and cross-sections 3×3.2 mm, were machined from a composite block in such a way that the longitudinal specimen axes were parallel to the plane in which the long axes of fibres are preferentially situated. The constant stress tensile creep tests were carried out

at temperatures from 373 to 673 K, and with the testing temperature continuously monitored and maintained constant to within ± 0.5 K of the desired value. The applied stress ranged from 15 to 200 MPa. The creep tests were performed in purified argon in tensile creep testing machines, making it possible to keep the nominal stress constant to within 0.1 % up to a true strain of about 0.35. The creep elongations were measured using a linear variable differential transducer and they were continuously recorded digitally and computer processed. Almost all of the specimens were run to final fracture.

Following creep testing, samples were prepared for examination by transmission electron microscopy (TEM). Observations were performed using a Philips CM 12 STEM transmission electron microscope with an operating voltage of 120 kV. Fractographic details were investigated by means of light microscopy and scanning electron microscopy (Philips SEM 505 microscope).

3. Results and discussion

3.1 Creep behaviour in monolithic and discontinuous fibre-reinforced AZ91 alloy

Representative creep data of the AZ91 alloy and the AZ91-20vol.%Al_2O_3(f) composite are shown in Fig. 1 for tests conducted at the two temperatures 423 and 473 K, respectively, where the minimum creep rate $\dot{\varepsilon}_m$ is plotted against the applied stress σ on a logarithmic scale. Inspection of Fig. 1 leads to two observations. First, the composite exhibits improved creep resistance by comparison with the monolithic alloy over the entire stress range used experimentally; the minimum creep rate for the composite is about two to three orders of magnitude less than that of the unreinforced alloy. Second, as depicted in Fig. 1, the stress dependences of the minimum creep rates for both materials are different in trend, which is clearly demonstrated by the characteristic curvatures on the curves at low stresses. While the slopes and therefore the apparent stress exponent $n = (\partial \ln \dot{\varepsilon} / \partial \ln \sigma)_T$ for the alloy decrease slightly with decreasing applied stress, the curvatures for the composite increase with decreasing applied stress.

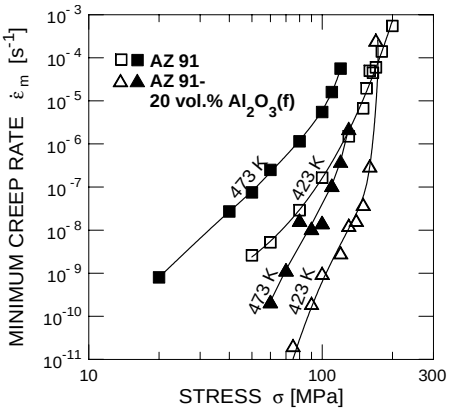

Fig. 1. Minimum creep rate versus stress for the AZ91 alloy and the composite.

The increase in n at the lower stresses in the composite is a fundamental

property of many metal matrix composites [23] and it is generally associated with the presence of a threshold stress marking a lower limiting stress below which no measurable strain rate can be achieved [24]. The data for the monolithic alloy suggest a transition to a value of n close to ~ 3 at the lower stress levels and this is consistent with earlier analyses of creep data for a composite with an AZ91 matrix [16] and data for an unreinforced AZ91 alloy [2, 6]. It is consistent also with results obtained recently on the unreinforced AZ91 alloy using acoustic emission [25]. A value of $n = 3$ suggests that viscous glide is the rate-controlling mechanism in the matrix alloy and the increase in n at the higher stresses is then due to the breakaway of the dislocations from their solute atmospheres [26].

3.2 Microstructural processes in creep

The detailed microstructural investigations on the crept AZ91 alloy and the AZ91-20vol.%Al_2O_3(f) composite have been reported in our previous papers [12, 17, 18]. The microstructure of the squeeze cast AZ91 alloy consists of the β-phase ($Mg_{17}Al_{12}$ and/or $Mg_{17}(Al, Zn)_{12}$) intermetallic compounds in a matrix of α magnesium solid solution. The microstructure of the AZ91-20vol.%Al_2O_3(f) composite is more complex than that of the unreinforced matrix alloy [27]. The most frequent morphology of the β-phase precipitates in the composite is coherent $Mg_{17}Al_{12}$ platelets. The significant microstructural changes in the composite observed after creep are a coarsening of the continuous β-phase and a partial dissolution of the massive β-phase. This dissolution is probably responsible for an additional continuous precipitation of fine $Mg_{17}Al_{12}$ particles which has been observed during the creep of the composite (Fig. 2). An apparent increase in the dislocation density in the composite, especially in the vicinity of the fibres, is almost certainly caused by the thermal mismatch between the fibres and the matrix.

Creep behaviour in the composite may be substantially influenced by the development of creep damage and fracture processes. Fractographic investigations of the composite failed to reveal either substantial creep fibre cracking and breakage or any debonding at the interfaces between the fibres and matrix due to creep at the lower applied stresses (Fig. 3). This result is supported by the response observed through acoustic emission monitored during the creep testing of the AZ91-20vol.%Al_2O_3(f) composite [25].

3.3 Threshold stress in the composite

Two procedures are available for estimating the magnitudes of the threshold stresses in high temperature creep [28–30]. In the first procedure, the creep data are extrapolated directly from the plots of the creep rate $\dot{\varepsilon}_m$ versus the applied stress σ to a lower limiting strain rate where the lines become vertical, typically at a strain rate of the order of 10^{-10} s^{-1} [29, 30]. In the second procedure, known

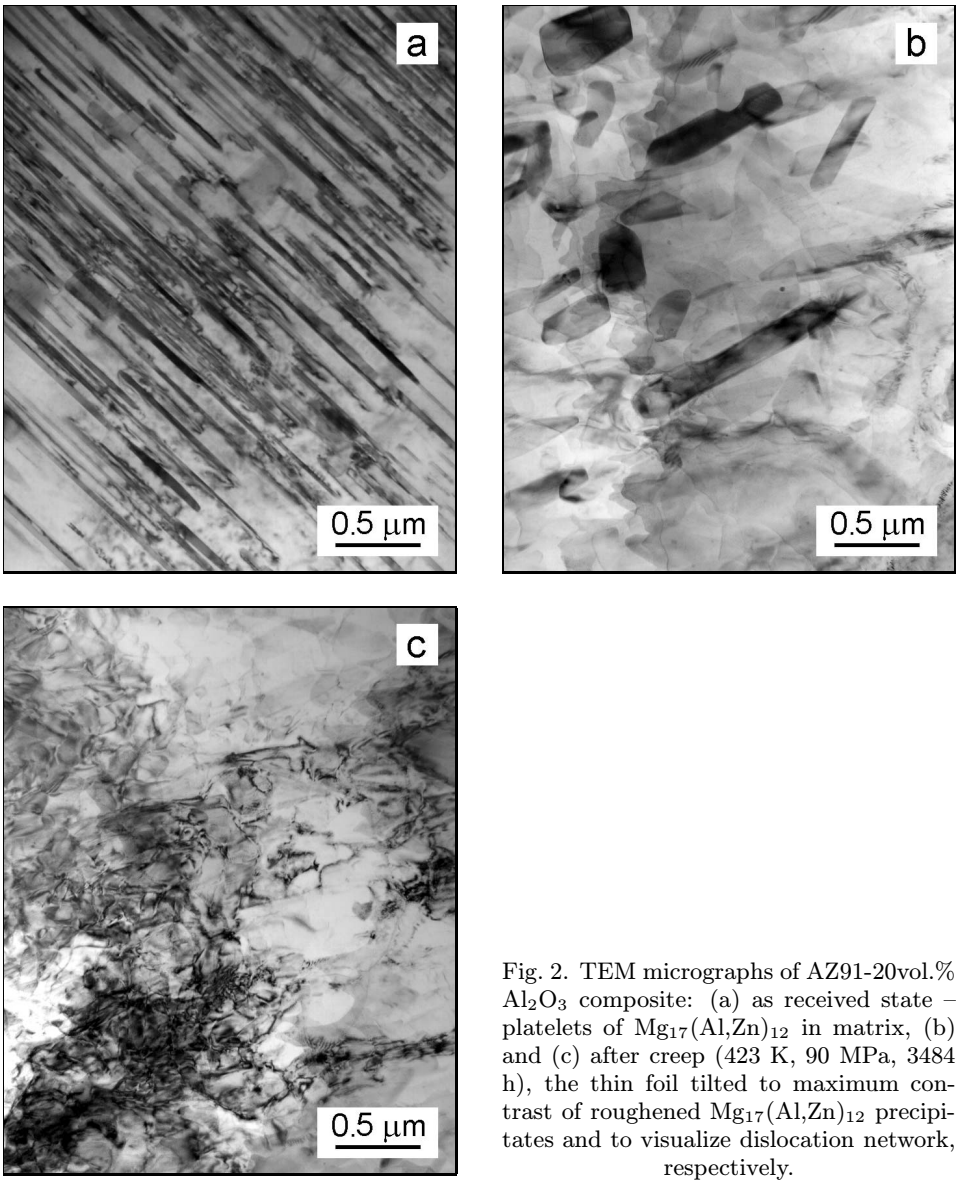

Fig. 2. TEM micrographs of AZ91-20vol.% Al_2O_3 composite: (a) as received state – platelets of $Mg_{17}(Al,Zn)_{12}$ in matrix, (b) and (c) after creep (423 K, 90 MPa, 3484 h), the thin foil tilted to maximum contrast of roughened $Mg_{17}(Al,Zn)_{12}$ precipitates and to visualize dislocation network, respectively.

as the linear extrapolation method, possible values of the stress exponent n are selected in advance and the creep data are replotted on linear axes in the form of the creep rate raised to the power of $1/n$ against the applied stress [28]. In practice, it has been shown that both of these procedures give consistent values for the threshold stress [31].

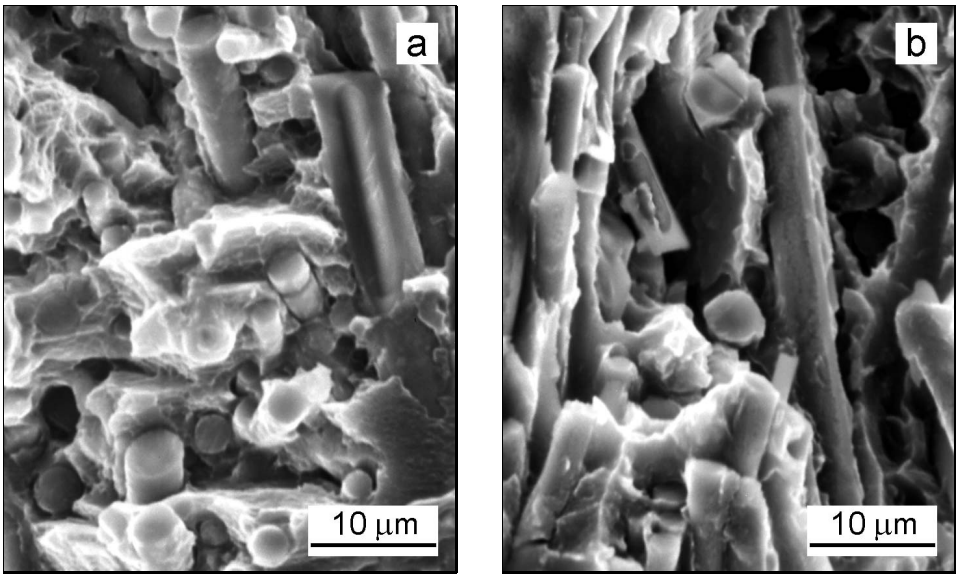

Fig. 3. SEM micrographs of AZ91-20vol.%Al_2O_3 composite taken at two different places, (a) and (b), of the creep fracture surface after testing at 473 K and stress 70 MPa.

Following the first procedure, the minimum creep rates $\dot{\varepsilon}_\mathrm{m}$ are plotted against applied stress σ in double logarithmic coordinates in Fig. 4. The shapes of the $\dot{\varepsilon}_\mathrm{m}(\sigma)$ relations exhibit a characteristic curvature for the true threshold creep behaviour. However, the curves through the individual datum points are not vertical at a creep rate of 10^{-10} s^{-1}. It should be stressed that this strain rate represents essentially the slowest rate which may be conveniently measured in laboratory experiments [30]. Further, Čadek and Šustek [29] proposed that it is necessary to obtain experimental data over not less than five orders of magnitude of creep rate in order to identify the appropriate values of σ_TH. This prerequisite can be hardly fulfilled for the investigated composite due to the occurrence of sudden fracture at creep rates of the order of 10^{-7} s^{-1} at all test-

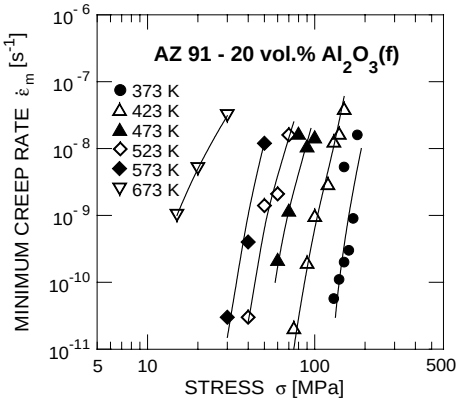

Fig. 4. Stress dependence of minimum creep rate for AZ91-20vol.%Al_2O_3(f) composite at various temperatures.

ing temperatures. Nevertheless, in order to check the use of this procedure, the stresses associated with a strain rate of 10^{-11} s^{-1} were read from the curves in Fig. 4 and these extrapolated values will be used in a later analysis.

Having only a small number of experimental points delineating the occurrence of an increase in n at the very lowest stresses in Fig. 4, it was appropriate to make use of the second procedure. In this procedure, it is possible to estimate the magnitude of σ_{TH} by plotting the data on linear axes as $\dot{\varepsilon}^{1/n}$ against σ and linearly extrapolating the data to give the threshold stresses at a zero strain rate [28]. A plot of this type requires, a priori, a judicious selection of the appropriate value of the true stress exponent, n. Analyses are usually undertaken using values of 3, 5 and 8, where these values are taken to represent the processes of viscous glide, high temperature climb controlled by lattice self-diffusion or a constant-structure model of creep controlled by lattice self-diffusion, respectively [29, 30]. The relations between $\dot{\varepsilon}^{1/n}$ and σ in double linear coordinates are shown in Fig. 5a,b for values of n of 3 and 5, respectively. It can be seen that for values of 3 and 5 of the true stress exponent, the $\dot{\varepsilon}^{1/n}$ vs. σ plots can be well fitted by straight lines for almost all the testing temperatures (the experimental datum points are fairly scattered at the lowest temperature of 373 K). However, detailed inspection of the individual plots shows that a true stress exponent of 3 yields the best linear fit – Fig. 5a. Figure 6 summarizes the values of the true threshold stresses determined using Fig. 5a with $n = 3$ and the extrapolation shown earlier in Fig. 4. Good agreement between the threshold stress values confirms the validity of both procedures and justifies the use of a value of 3 for the true stress exponent in Fig. 5a. Figure 6 shows

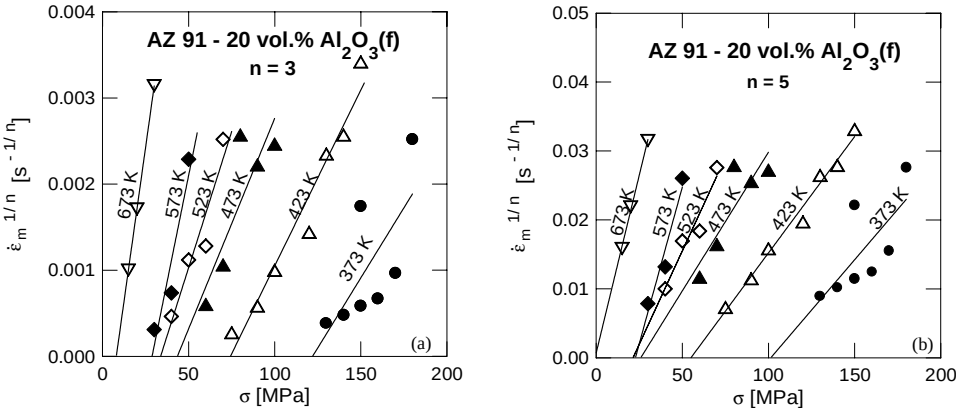

Fig. 5. The linear extrapolation procedure for determining the threshold stress in the composite at various temperature using values of stress exponent n of (a) 3, (b) 5, respectively.

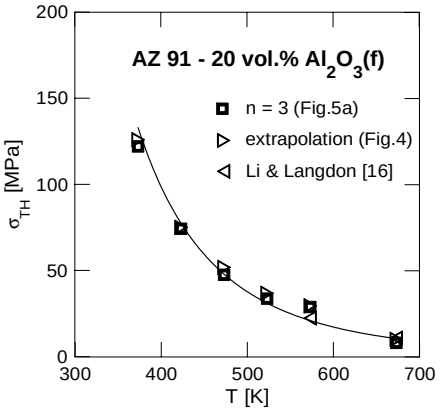

Fig. 6. Temperature dependence of the threshold stress σ_{TH} in composite.

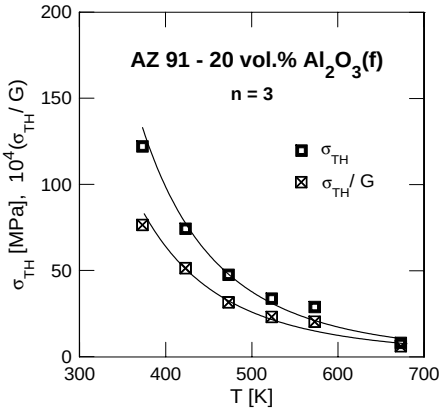

Fig. 7. Temperature dependence of the σ_{TH}/G ratio.

also the values of the threshold stress for temperatures of 573 and 673 K for an identical composite to that used in this work but creep tested using a double-shear configuration [16].

The finding of $n = 3$ over a wide range of effective stress provides support for adopting the suggestion [15–17, 19] that the AZ91 composite exhibits creep behaviour which is consistent with the behaviour anticipated for magnesium solid solution alloys [15, 16, 21]. Although the precise interpretation of the threshold stress is not well understood at the present time, several possible mechanisms are available to explain the origin of the threshold stress occurring in materials where mobile dislocations pass through arrays of particles [32]. In practice, the threshold stresses in the squeeze – cast AZ91-20vol.%Al_2O_3(f) composite probably arise from an attractive interaction between the mobile dislocations and $Mg_{17}(Al,Zn)_{12}$ precipitates occurring in the matrix lattice.

Figure 7 shows that the threshold stress decreases with increasing temperature more strongly than the matrix shear modulus, G. This result implies that the threshold stress values are closely connected with the development of a continuous precipitate morphology of $Mg_{17}(Al,Zn)_{12}$ particles (Fig. 2), the change in the volume and/or planar density of precipitates and the change in the matrix/precipitate orientation relationship. The strong temperature effect on the volume density of $Mg_{17}Al_{12}$ particles has been reported by Celotto [33]. The measured number of continuous precipitates per unit volume in aged AZ91 alloy decreased from 1.0×10^{12} mm^{-3} at 343 K to 1.5×10^{9} mm^{-3} at 573 K. It should be stressed that the change in the particle density and their shape can immediately influence the values of the interparticle spacing and thus the values of the threshold stresses.

3.4 Load transfer

Creep strengthening of the composite may occur by direct strengthening due to a load transfer from the matrix to the reinforcement. Thus, load transfer is accompanied by a redistribution of stresses in the matrix and this reduces the effective stress for creep.

In the presence of load transfer, the creep data may be successfully reconciled by taking, for the same loading conditions, the ratio of the creep rates of the composite, $\dot{\varepsilon}_c$, and the matrix alloy, $\dot{\varepsilon}_a$, equals to a factor that is given by $(1-\alpha)^n$, where α is the load-transfer coefficient having values lying within the range from 0 (where there is no load transfer) to 1 (where there is full transfer of the load) and n is the appropriate value of the stress exponent [34]. Thus, taking $n = 3$ and using the experimental data in Fig. 1, the values of α in the present investigation are estimated to lie within the range of ~ 0.8 (473 K) to ~ 0.9 (423 K), see Table 1. It is possible to check the validity of this approach by estimating a theoretical value for α by using the modified shear-lag model [35] and considering the load-transfer effect at the end of short fibres for various reinforcement geometries and arrangements (for example, the volume fraction of the fibres, their average aspect ratio, etc.) [35]. The values of α predicted theoretically from this model, assuming 20 vol pct of short-fibre reinforcement and an experimentally observed fibre aspect ratio given by a length/diameter value of ~ 50, are of the order of ~ 0.8. It follows, therefore, that the predicted values of α are in excellent agreement with the experimental values inferred from the present analysis.

Table 1. The values of load transfer coefficients α for $n = 3$ ($\dot{\varepsilon}_c/\dot{\varepsilon}_a = (1-\alpha)^n$)

T [K]	σ [MPa]	$\dot{\varepsilon}_c$ [s^{-1}]	$\dot{\varepsilon}_a$ [s^{-1}]	α
423	90	2.45×10^{-10}	1.10×10^{-7}	0.87
	100	6.97×10^{-10}	2.34×10^{-7}	0.86
	125	6.40×10^{-9}	1.15×10^{-6}	0.82
	150	3.90×10^{-8}	4.27×10^{-6}	0.79
473	50	7.50×10^{-11}	8.61×10^{-8}	0.90
	70	1.36×10^{-9}	5.48×10^{-7}	0.86
	90	1.18×10^{-8}	2.18×10^{-6}	0.82
	100	2.94×10^{-8}	3.89×10^{-6}	0.80

4. Conclusions

Creep deformation in a short-fibre AZ91 alloy-based composite is controlled by flow in the matrix and viscous glide is the rate-controlling mechanism. The

results indicate that the creep resistance of the composite is considerably improved compared to the matrix alloy due to the additional creep strengthening that is introduced in the monolithic alloy due to the short-fibre reinforcement. This additional strengthening may arise from the existence of the threshold stress, a load transfer effect and/or a substructural strengthening effect because of the thermal mismatch between the matrix and the reinforcement.

Acknowledgements

Financial support for this work was provided by the Grant Agency of the Czech Republic – Czech Science Foundation under the Grant Project 106/03/0901.

REFERENCES

[1] MILLER, W. K.: Metall. Trans., *A22*, 1991, p. 873.
[2] BLUM, W.—WEIDINGER, P.—WATZINGER, B.—SEDLACEK, R.—RÖSCH, R.—HALDENWANGER, Z.: Z. Metallkd., *88*, 1997, p. 636.
[3] DARGUSH, M. S.—DUNLOP, G. L.—PETTERSEN, K.: In: Magnesium Alloys and Their Applications. Eds.: Mordike, B. L., Kainer, K. U. Frankfurt, Werkstoff-Informationgesellschaft 1998, p. 277.
[4] REGEV, M.—AGHION, E.—ROSEN, A.: Mater. Sci. Eng. A, *A234–236*, 1997, p. 123.
[5] PAHUTOVÁ, M.—BŘEZINA, J.—KUCHAŘOVÁ, K.—SKLENIČKA, V.—LANGDON, T. G.: Mater. Letters, *39*, 1999, p. 179.
[6] SKLENIČKA, V.—PAHUTOVÁ, M.—KUCHAŘOVÁ, K.—SVOBODA, M.—LANGDON, T. G.: Key Eng. Mater., *171–174*, 2000, p. 593.
[7] REGEV, M.—BOTSTEIN, O.—ROSEN, A.: In: Magnesium 2000. Eds.: Aghion, E., Eliezer, D. Beer-Sheva, Israel, Magnesium Research Inst. 2000, p. 301.
[8] SPIGARELLI, S.—CABIBBO, M.—EVANGELISTA, E.—REGEV, M.—ROSEN, A.: ibid, p. 293.
[9] PAHUTOVÁ, M.—SKLENIČKA, V.—KUCHAŘOVÁ, K.—BŘEZINA, J.—SVOBODA, M.—LANGDON, T. G.: ibid, p. 285.
[10] MORDIKE, B. L.—LUKÁČ, P.: In: 3rd Int. Magnesium Conference. Ed.: Lorimer, G. W. London, The Institute of Metals 1997, p. 419.
[11] SPIGARELLI, S.—REGEV, M.—EVANGELISTA, E.—ROSEN, A.: Mater. Sci. Technol., *17*, 2001, p. 627.
[12] SKLENIČKA, V.—PAHUTOVÁ, M.—KUCHAŘOVÁ, K.—SVOBODA, M.—LANGDON, T. G.: Metall. Mater. Trans., *33A*, 2002, p. 883.
[13] ROSEN, A.: In: Magnesium Alloys. Eds.: Aghion, E., Eliezer, D. Haifa, Israel, The Israeli Consortium for the Development of Magnesium Technology 2004, p. 45.
[14] SKLENIČKA, V.—PAHUTOVÁ, M.—KUCHAŘOVÁ, K.—SVOBODA, M.—KAINER, K. U.: Mater. Sci. Forum, *419–422*, 2003, p. 805.
[15] LI, Y.—SKLENIČKA, V.—LANGDON, T. G.: In: Creep Behaviour of Advanced Materials for the 21st Century. Eds.: Mishra, R. S. et al. Warendale, USA, TMS 1999, p. 171.
[16] LI, Y.—LANGDON, T. G.: Metall. Mater. Trans. A., *30A*, 1999, p. 2059.
[17] SKLENIČKA, V.—SVOBODA, M.—PAHUTOVÁ, M.—KUCHAŘOVÁ, K.—LANGDON, T. G.: Mater. Sci. Eng. A., *A319–321*, 2001, p. 741.

[18] SVOBODA, M.—PAHUTOVÁ, M.—KUCHAŘOVÁ, K.—SKLENIČKA, V.—LANGDON, T. G.: Mater. Sci. Eng. A., *A324*, 2002, p. 151.
[19] PAHUTOVÁ, M.—SKLENIČKA, V.—KUCHAŘOVÁ, K.—SVOBODA, M.: Int. J. of Materials & Product Technology, *18*, 2003, p. 116.
[20] SKLENIČKA, V.—LANGDON, T. G.: J. Mater. Sci., *39*, 2004, p. 1647.
[21] VAGARALI, S. S.—LANGDON, T. G.: Acta Metall., *30*, 1982, p. 1157.
[22] PARK, K.-T.—LAVERNIA, E. J.—MOHAMED, F. A.: Acta Metall. Mater., *38*, 1990, p. 2149.
[23] LI, Y.—LANGDON, T. G.: Metall. Mater. Trans., *30A*, 1999, p. 315.
[24] GIBELING, J. C.—NIX, W. D.: Mater. Sci. Eng., *45*, 1980, p. 123.
[25] CHMELÍK, F.—LUKÁČ, P.—JANEČEK, M.—MOLL, F.—MORDIKE, B. L.—KAINER, K. U.—LANGDON, T. G.: Mater. Sci. Eng., *A338*, 2002, p. 1.
[26] YAVARI, P.—LANGDON, T. G.: Acta Metall., *30*, 1982, p. 2181.
[27] KIEHN, J.—KAINER, K. U.—VOSTRÝ, P.—STULÍKOVÁ, I.: Phys. Stat. Sol. (a), *161*, 1997, p. 85.
[28] LAGNEBORG, R.—BERGMAN, B.: Metal Sci., *10*, 1976, p. 20.
[29] ČADEK, J.—ŠUSTEK, V.: Scripta Metall. Mater., *30*, 1994, p. 277.
[30] LI, Y.—LANGDON, T. G.: Scripta Mater., *36*, 1997, p. 1457.
[31] LI, Y.—LANGDON, T. G.: Metall. Mater. Trans., *28A*, 1997, p. 1271.
[32] GIBELING, J. C.: In: Creep Behavior of Advanced Materials for the 21st Century. Eds.: Mishra, R. S. et al. Warrendale, USA, TMS 1999, p. 239.
[33] CELOTTO, S.: Acta Mater., *48*, 2000, p. 1775.
[34] PARK, K. T.—LAVERNIA, E. J.—MOHAMED, F. A.: Acta Metall. Mater., *42*, 1994, p. 667.
[35] NARDONE, V. C.—PREWO, K. M.: Scripta Metall., *20*, 1986, p. 43.